Supplementary Information

Atomic-level Insights into the Highly Conductive Lithium Thiophosphate Solid Electrolytes with Exceptional Stability Against Lithium Metal

Huseyin Sener Sen*, Bora Karasulu*

Department of Chemistry, University of Warwick, Coventry CV4 7AL, U.K.

Table of Contents

The Workflow for Interface Generation

The interface structures were generated following a systematic approach. First, the bulk structures of both materials were fully relaxed to ensure optimized geometries before constructing surface slabs. Surface terminations were selected while maintaining the stoichiometry, and multiple Miller indices were considered to explore different possible orientations. The stability of these surfaces was assessed by computing their formation energies, allowing us to identify the most favourable configurations. The selected slabs were then aligned (in ab-plane) and stacked along the c-axis, applying affine transformations to minimize lattice mismatch while maximizing interfacial contact. To ensure the structural accuracy of the constructed interfaces, a final relaxation step was performed, optimizing atomic positions and evaluating key interfacial properties such as adhesion energy and stability. This computational workflow process was automated within the INTERFACER code, which streamlines interface generation and facilitates high-throughput screening of interfacial structures.

Table S1. Calculated tracer diffusivity (D*), total mean square displacement (TMSD), averaged distance between neighbouring mobile-ion sites (a), total effective ion hops (N_{eff}) and relative standard deviation (RSD) as discussed in other works.[1,2]

	D* (cm^2/s)	TMSD ($Å^2$)	a (Å)	N_{eff}	RSD
$Li_7P_3S_{11}$	10.4 x 10^{-6}	2058	2.7	282.33	0.24
Li_5PS	3.2 x 10^{-6}	4898	2.39	857.55	0.16
Li_7PS_2	1.2 x 10^{-6}	1699	2.39	297.40	0.24
Li_8P_2S	2.8 x 10^{-6}	3793	2.5	606.91	0.18
$Li_{11}P_3S$	1.1 x 10^{-6}	1850	2.53	288.96	0.24
γ-Li_3PS_4	1.4 x 10^{-7}	731	2.77	95.31	0.39
β-Li_3PS_4	1.5 x 10^{-6}	989	3.04	106.99	0.37

Calculation of Relative Standard Deviation[1]

TMSD over time interval Δt is calculated from MSD as; $TMSD(\Delta t) = MSD(\Delta t) * N$, where N is the number of mobile ions (charge carriers), which in our case are the Li atoms. N_{eff} is the effective number of ion hops that contributed to the TMSD in the entire duration of the MD simulation which can be calculated as $N_{eff} = \frac{\max(TMSD(\Delta t))}{a^2}$, where $\max(TMSD(\Delta t))$ is the maximum value of $TMSD(\Delta t)$ and a is the average distance between neighbouring mobile-ion sites. Then, the relative standard deviation (RSD) of the diffusion constant can be calculated using an empirical relation as follows; $RSD = \frac{3.43}{N_{eff}} + 0.04$.

For AIMD simulations with $0.2 <$ RSD < 0.5 is reasonable but still may have a notable statistical error for estimated diffusivity. The simulations for $Li_7P_3S_{11}$, Li_7PS_2, $Li_{11}P_3S$, γ-Li_3PS_4 and β-Li_3PS_4 are in this category. The simulations for Li_5PS and Li_8P_2S have RSD below 0.2 which are statistically more representative. This means, the relative error in diffusivity is minimized for Li_5PS and Li_8P_2S.

Table S2. Calculated chemical potentials from different sets of subsystems.

	μ_{Li} (eV)	**μ_P (eV)**	**μ_S (eV)**
Set 1: bcc-Li, Li_2S, Li_3P	-1.90	-8.23	-8.17
Set 2: Li_2S, Li_3P, P_2S_5	-3.44	-3.60	-5.09
Set 3: bcc-Li, bulk S, bulk P	-1.90	-5.38	-4.13

Table S3. Calculated formation energies per formula unit of the studied systems using the chemical potentials from Table S2.

(eV)	Set 1	Set 2	Set 3
bcc-Li	0.0	1.54	0.0
Li_3P	0.0	0.0	-0.71
γ-Li_3PS_4	1.43	-0.11	-0.95
$Li_7P_3S_{11}$	1.68	-0.09	-0.85
Li_2S	0.0	0.0	-1.35
Li_7PS_2	0.04	0.04	-1.05
Li_5PS	0.05	0.05	-0.93
Li_8P_2S	0.04	0.04	-0.85
$Li_{11}P_3S$	0.03	0.03	-0.81
P_2S_5	3.53	0.0	-0.17

Table S4. The calculated decomposition and intrinsic electrochemical stability windows (DESW and IESW, respectively) for ternary solid electrolytes.

	Decomposition		Intrinsic	
Ternary	DESW (V)	Decomposition Reaction	IESW (V)	Delithiation Reaction
Li_7PS_2	0 – 0.87	$Li_7PS_2 \rightarrow 2Li + 2Li_2S + LiP$	0 – 1.50	$8Li_7PS_2 \rightarrow 56Li + P_4S_9 + P_4S_7$
Li_5PS	0 – 0.87	$Li_5PS \rightarrow 2Li + Li_2S + LiP$	0 – 1.27	$16Li_5PS \rightarrow 80Li + 3P_4S_3 + P_4S_7$
Li_8P_2S	0 – 0.87	$Li_8P_2S \rightarrow 4Li + Li_2S + 2LiP$	0 – 1.18	$3Li_8P_2S \rightarrow 24Li + P_4S_3 + 2P$
$Li_{11}P_3S$	0 – 0.87	$Li_{11}P_3S \rightarrow 6Li + Li_2S + 3LiP$	0 – 1.15	$3Li_{11}P_3S \rightarrow 33Li + P_4S_3 + 5P$

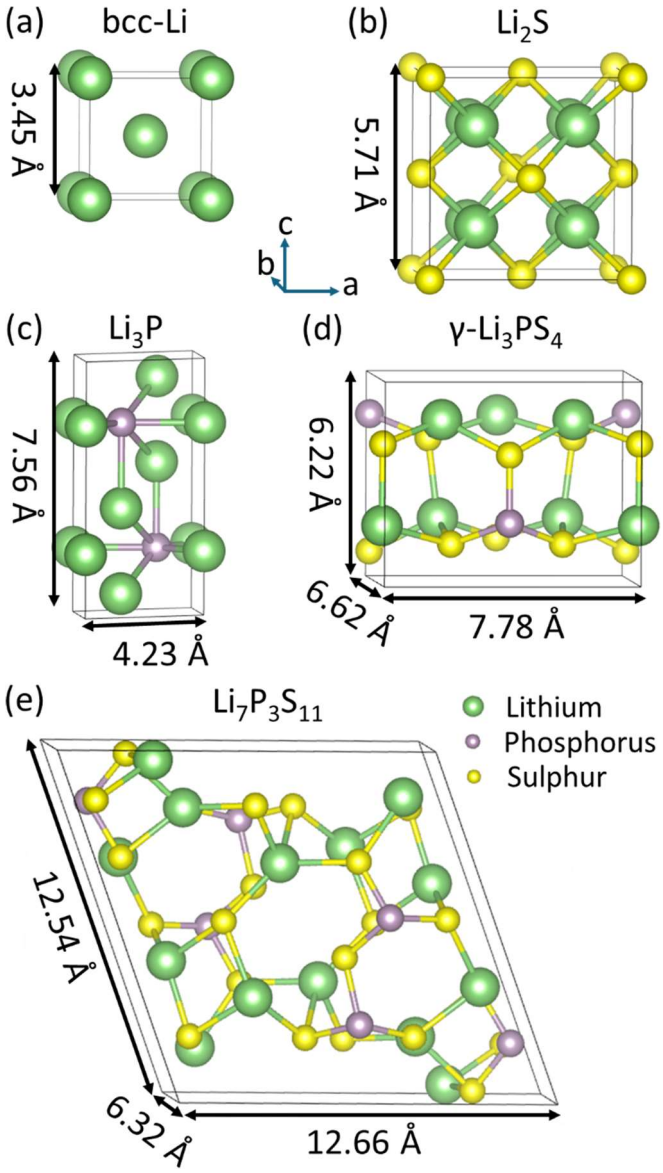

Figure S1. Unit cells for a) bcc-Li, b) Li_2S, c) Li_3P, d) γ-Li_3PS_4, and e) $Li_7P_3S_{11}$. Green, purple and yellow spheres represent Li, P and S atoms, respectively.

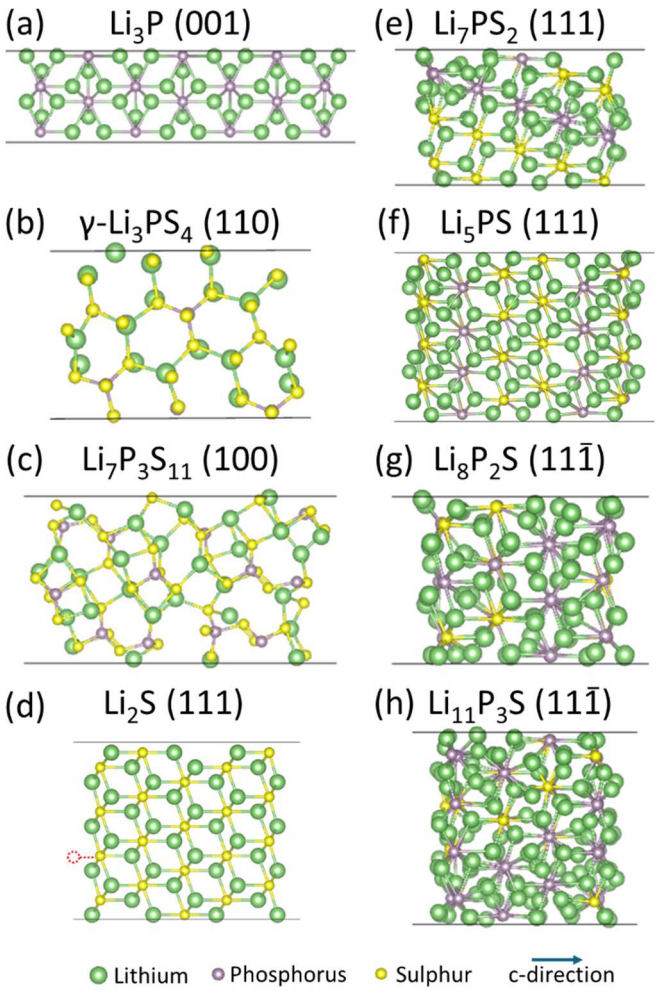

Figure S2. Energetically the most favourable surfaces. a) Li_3P (100), b) γ-Li_3PS_4 (110), c) $Li_7P_3S_{11}$ (100), d) Li_2S (111), e) Li_7PS_2 (111), f) Li_5PS (111), g) Li_8P_2S (11$\bar{1}$), and g) $Li_{11}P_3S$ (11$\bar{1}$). Green, purple and yellow spheres represent Li, P and S atoms, respectively.

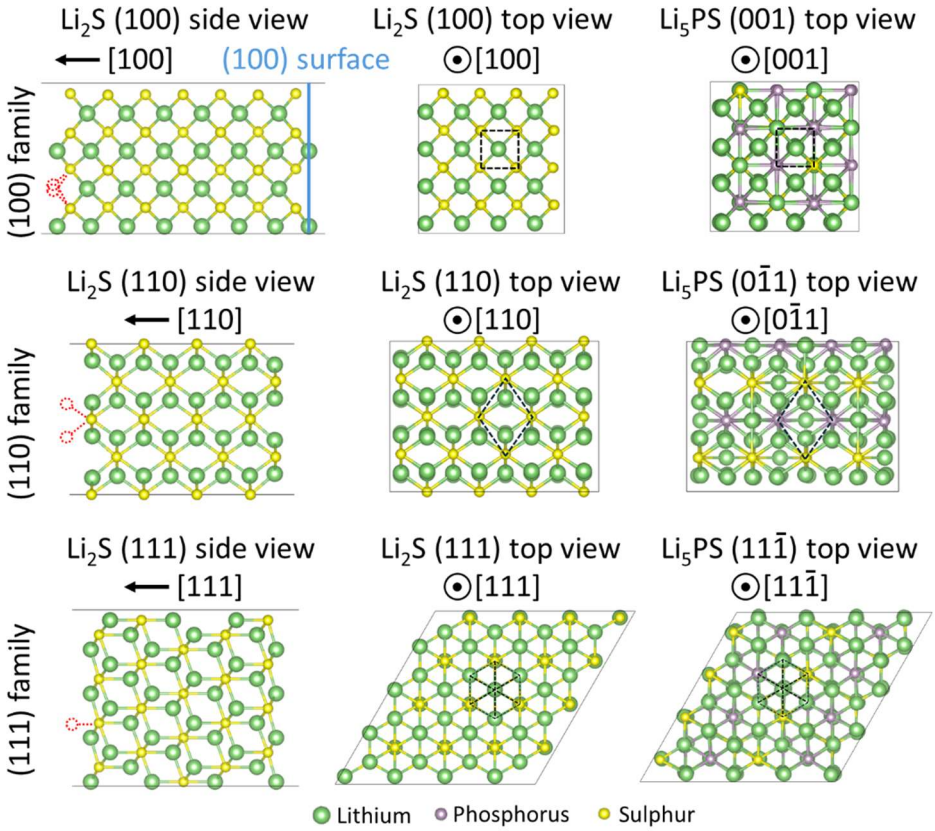

Figure S3. Three distinct families of surfaces as identified by their unique Miller indices for Li_2S and the new ternaries. The families can be distinguished by the structural motives they encompass. The red lines and circles represent Li-S bond and Li atoms lost due to cutting to form the surface.

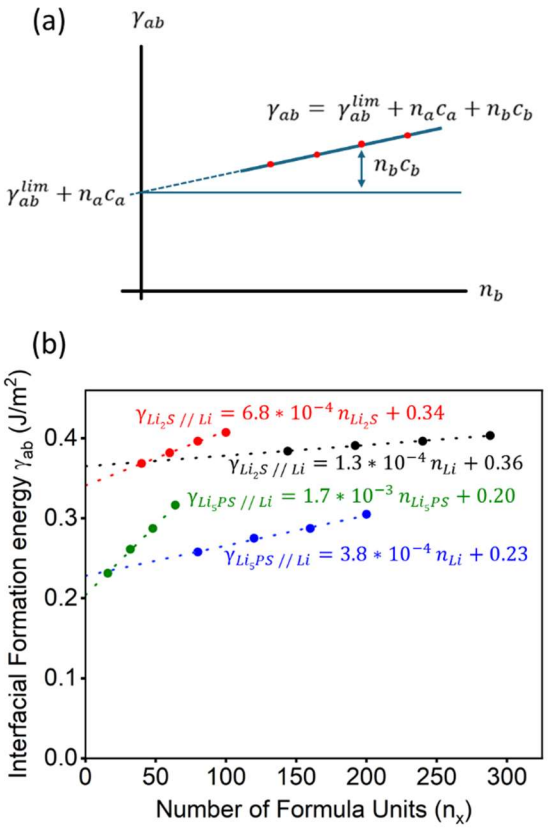

Figure S4. a) A schematic plot to illustrate the calculation of strain using **Eqn 10** (extrapolation method) via the linear change of interface formation energy as a function of the thickness of slab *b*. b) Linear dependence of the interface formation energy as a function of slab thickness for Li_2S // Li and Li_5PS // Li interface structures.

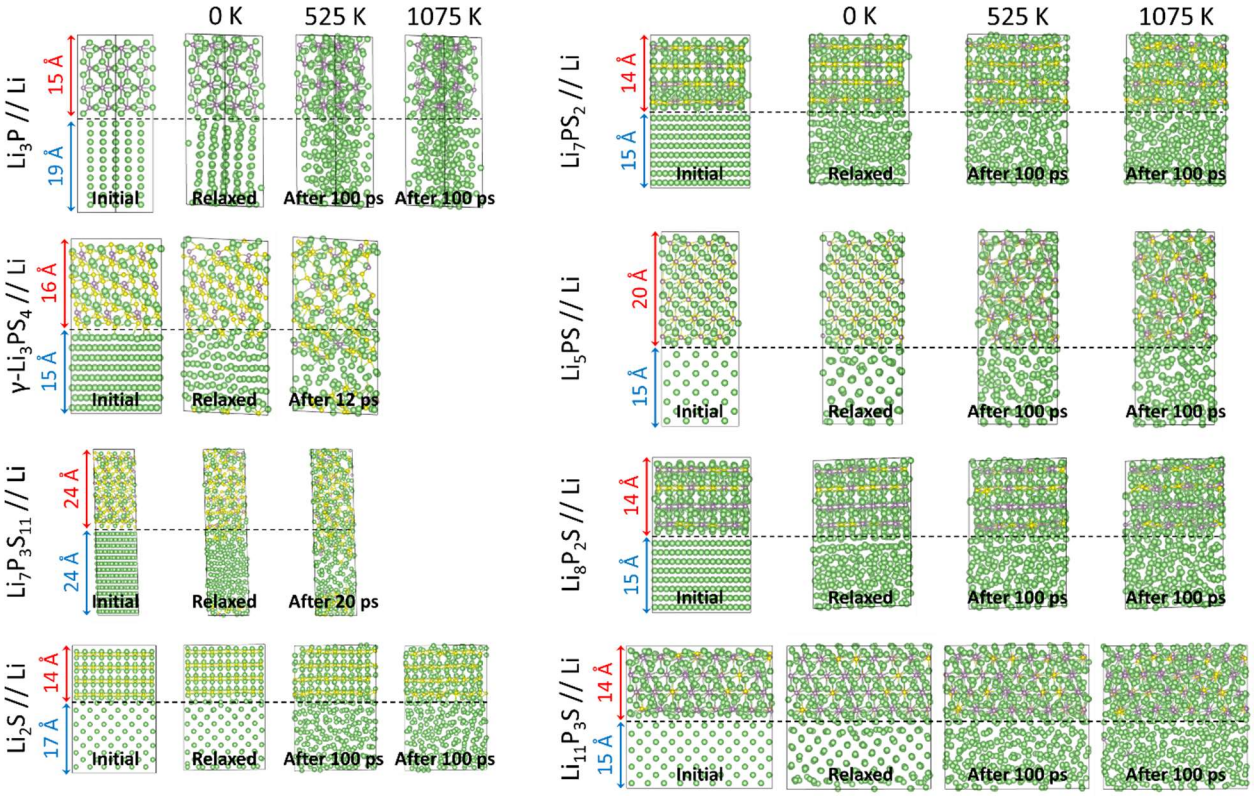

Figure S5. The evolution of studied interface structures. Initial (initially constructed structure by INTERFACER), Relaxed (fully DFT optimised structure – both lattice vectors and atomic positions – at 0 K) and After 100 ps (evolution of the structure during AIMD simulations at 525 K and 1075 K). The black dashed lines mark the initial position of the interface. Green, purple and yellow spheres represent Li, P and S atoms, respectively.

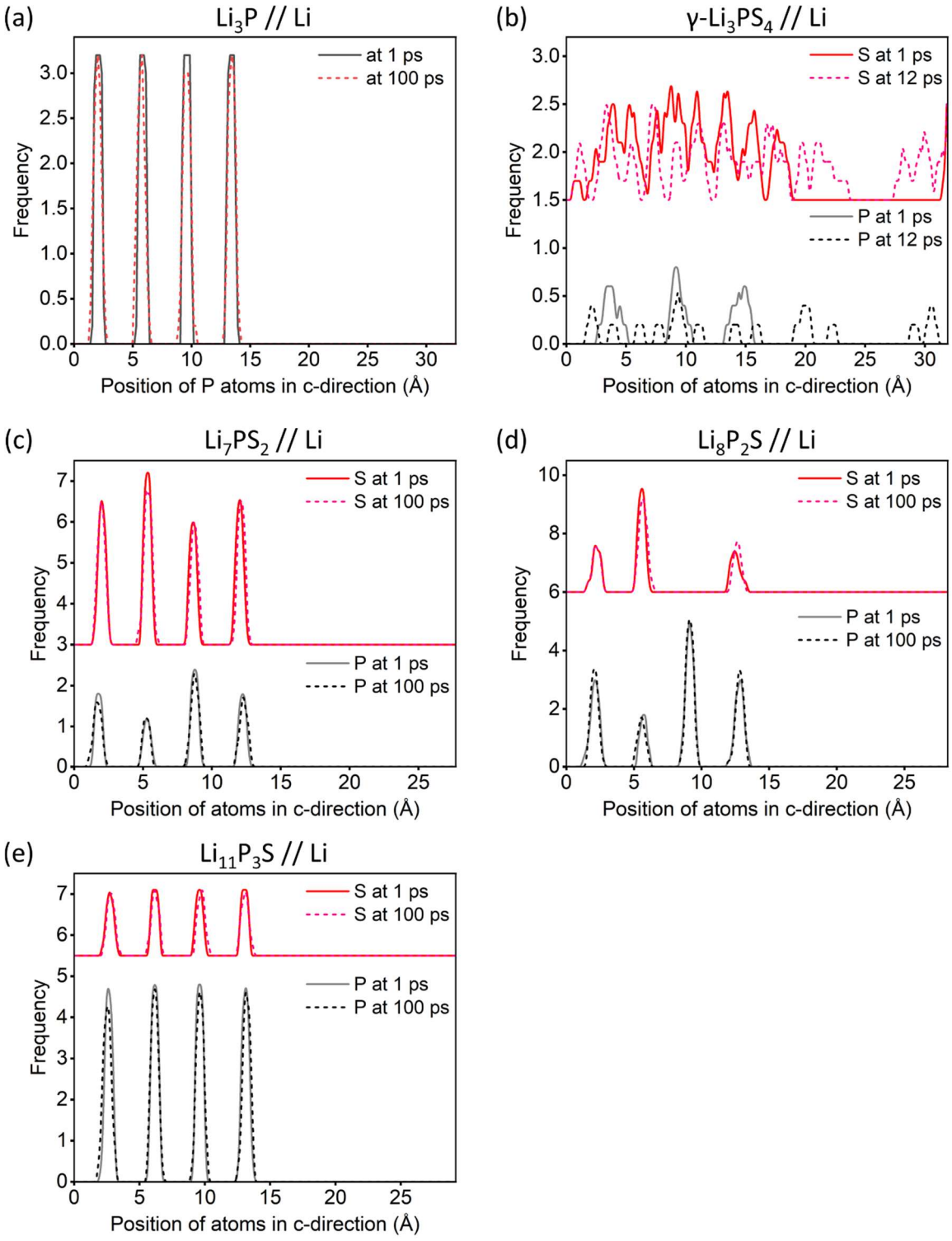

Figure S6. The positional histogram of P and S atoms along c-axis (perpendicular to the interface in a) Li_3P // Li, b) γ-Li_3PS_4 // Li, c) Li_7PS_2 // Li, d) Li_8P_2S // Li, and e) $Li_{11}P_3S$ // Li at certain time steps during AIMD simulation at 525 K.

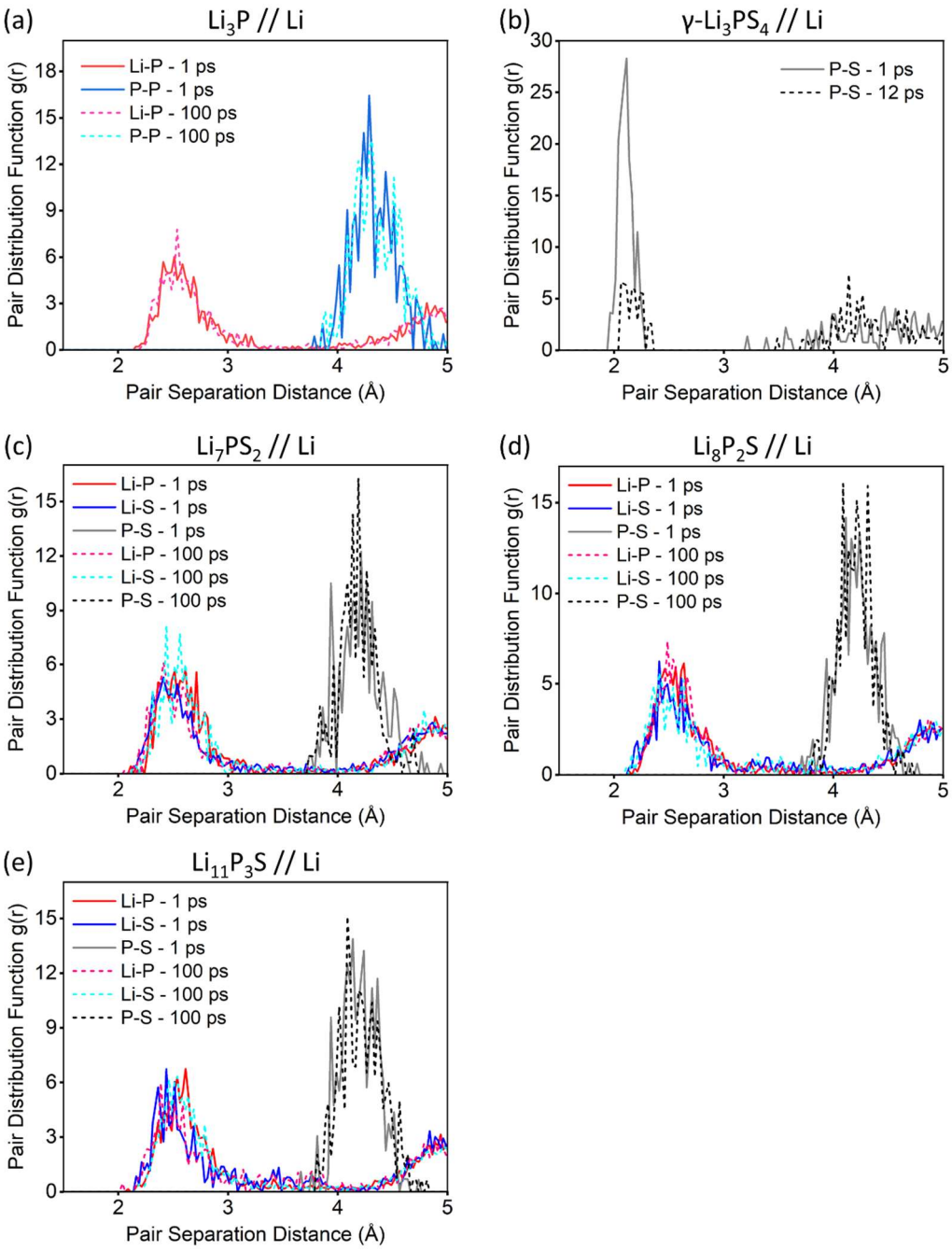

Figure S7. The pair distributions of certain atomic pairs in a) Li_3P // Li, b) γ-Li_3PS_4 // Li, c) Li_7PS_2 // Li, d) Li_8P_2S // Li, and e) $Li_{11}P_3S$ // Li at certain time steps during AIMD simulation at 525 K.

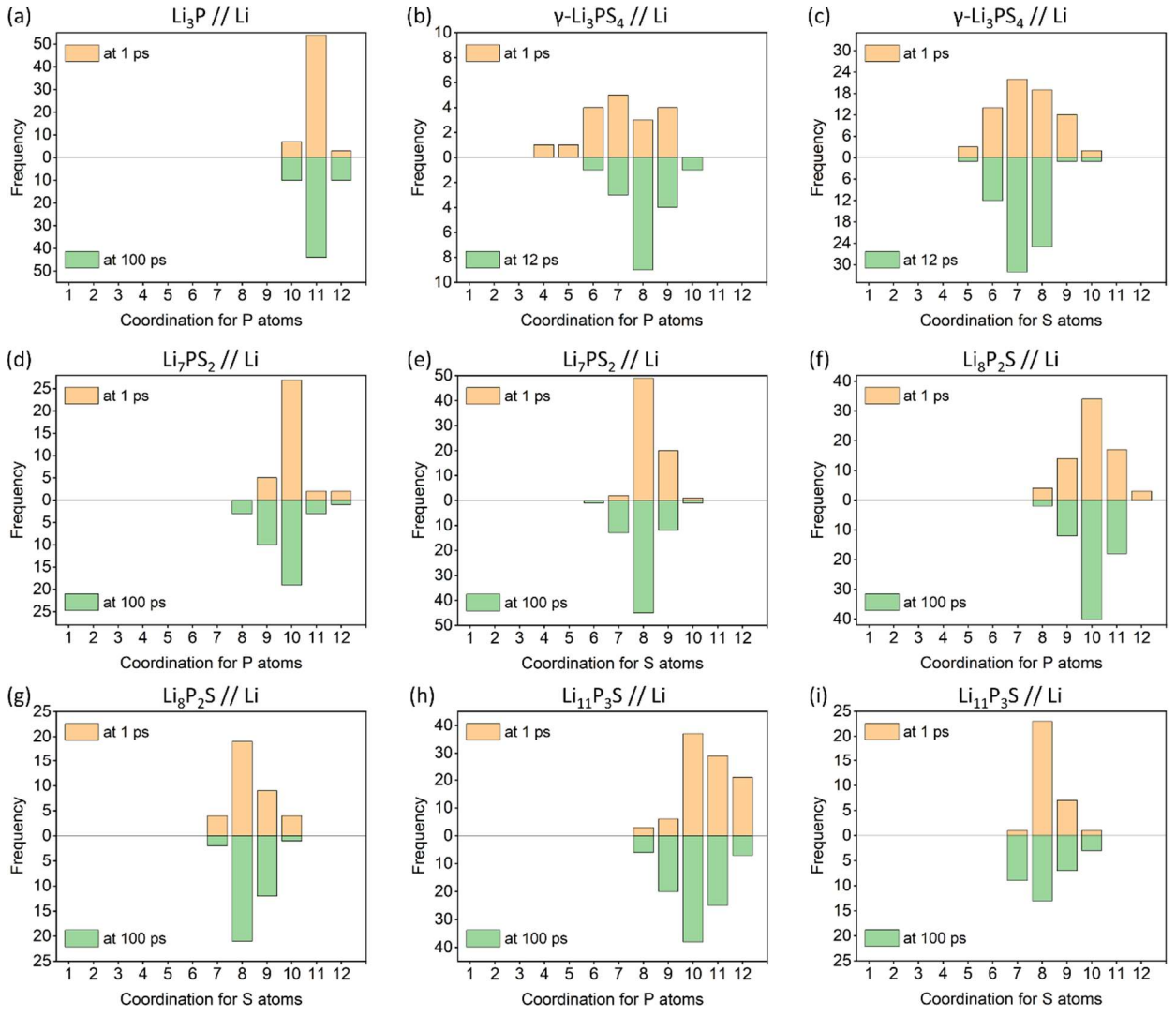

Figure S8. The coordination numbers for a) P atoms in Li_3P // Li, b) P atoms in γ-Li_3PS_4 // Li, c) S atoms in γ-Li_3PS_4 // Li, d) P atoms in Li_7PS_2 // Li, e) S atoms in Li_7PS_2 // Li, f) P atoms in Li_8P_2S // Li, g) S atoms in Li_8P_2S // Li, i) P atoms in $Li_{11}P_3S$ // Li, and i) S atoms in $Li_{11}P_3S$ // Li at certain time steps during AIMD simulation at 525 K.

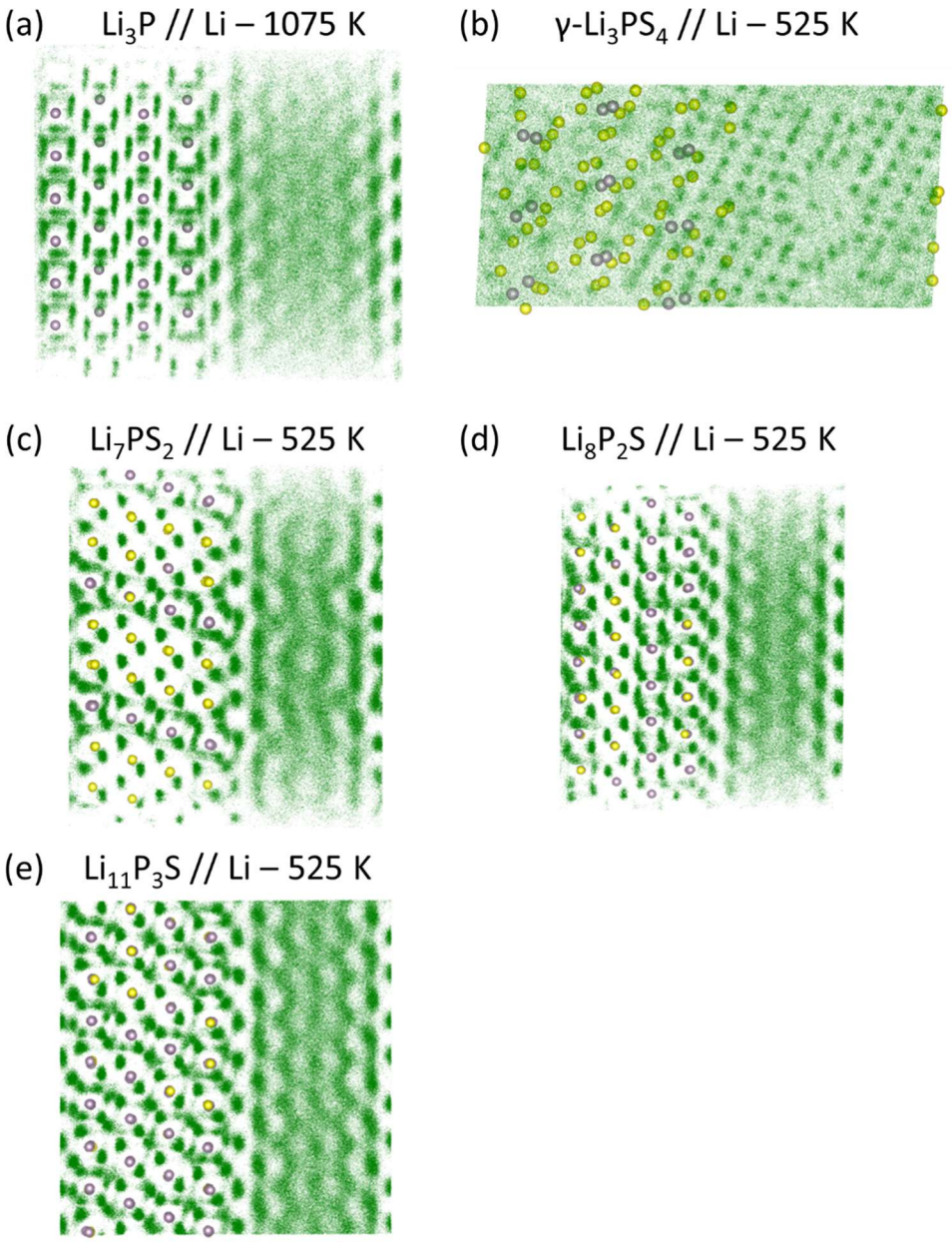

Figure S9. Li^+-ion trajectory (green) for a) Li_3P // Li at 1075 K, b) γ-Li_3PS_4 // Li at 525 K, c) Li_7PS_2 // Li at 525 K, d) Li_8P_2S // Li at 525 K, e) $Li_{11}P_3S$ // Li at 525 K. The positions of the phosphorus (purple) and sulphur (yellow) atoms at time t = 0 ps are shown in the background.

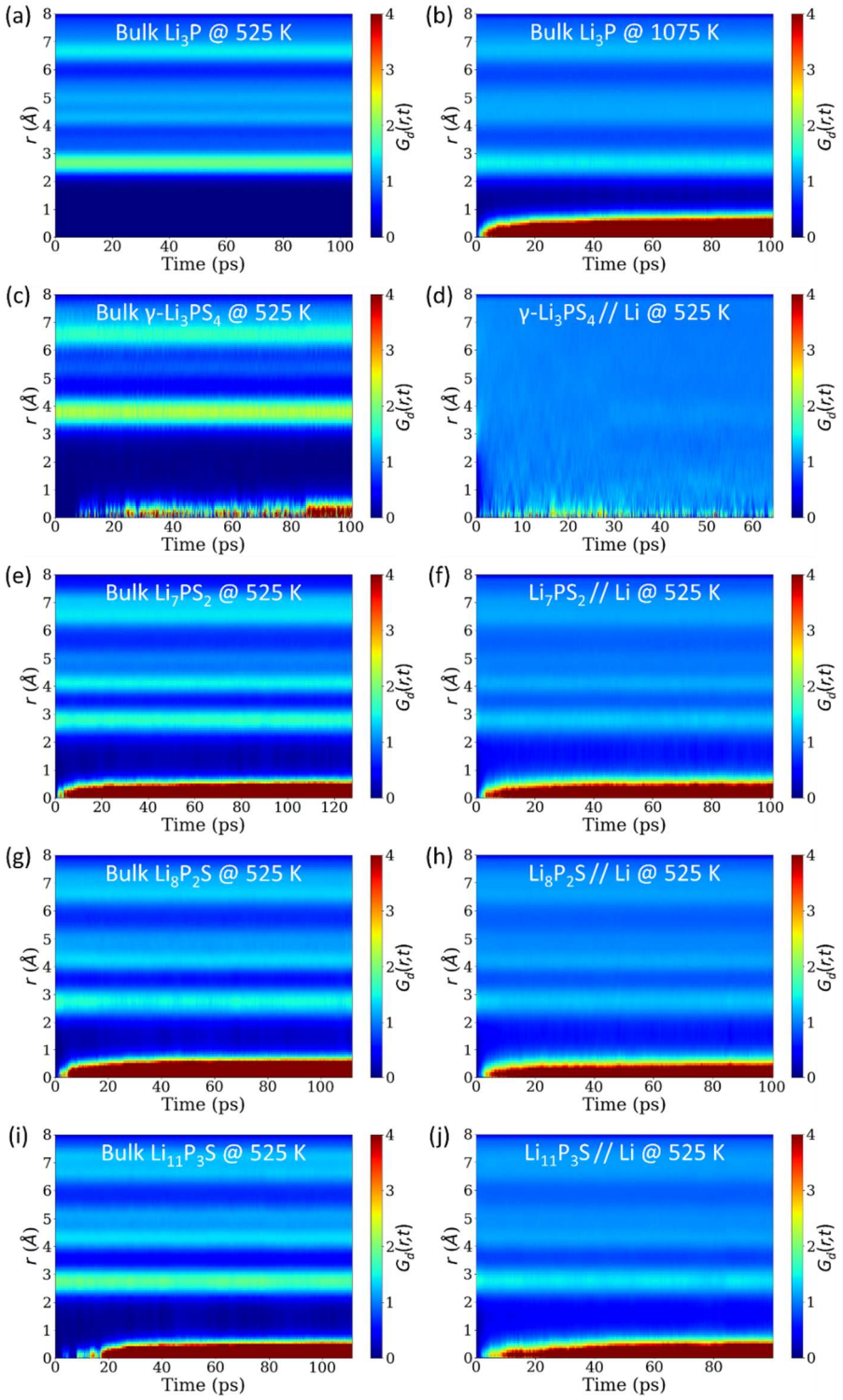

Figure S10. The distinct part of the Van Hove correlation function for Li atoms in a) bulk Li_3P at 525 K, b) bulk Li_3P at 1075 K, c) bulk γ-Li_3PS_4 at 525 K, d) γ-Li_3PS_4 // Li at 525 K, e) Li_7PS_2 at 525 K, f) Li_7PS_2 // Li at 525 K, g) Li_8P_2S at 525 K, h) Li_8P_2S // Li at 525 K, i) $Li_{11}P_3S$ at 525 K and, j) $Li_{11}P_3S$ // Li at 525 K.

References

1. X. He, Y. Zhu, A. Epstein and Y. Mo, *NPJ Comput Mater*, 2018, **4**, 18.

2. M. K. Gupta, R. Mittal, B. Singh, O. Delaire, S. N. Achary, S. Rols, A. K. Tyagi and S. L. Chaplot, *Phys Rev B*, 2021, **103**, 174109.